U.S. Department
of Transportation

Federal Highway
Administration

Publication No. FHWA-RD-90-111
August 1993

Blowup of a Concrete Pavement Adjoining a Rigid Structure

Research and Development
Turner-Fairbank Highway Research Center
6300 Georgetown Pike
McLean, Virginia 22101-2296

FOREWORD

There is general agreement that pavement blowups are caused by axial compression forces induced in the pavement by a rise in temperature and moisture, and that they usually occur at traverse joints or crack; although blowups ofa long continuously reinforced concrete pavement (CRCP) with a traverse "hinge" is equivalent to lift-off buckling of the pavement.[1] A related analysis was presented in 1985.[2]

This paper contains an analysis of the case when a long continuous reinforced concrete pavement is subjected to temperature and moisture increases and adjoins a rigid structure. The analysis is similar to the one used in reference 1. The closed form solutions are evaluated numerically. They are then compared with those of the jointless pavement analyzed previously, to show the effect of the rigid structure on pavement response.

This report will be of interest to researchers and engineers concerned with the assessment of blowups of concrete pavements.

Sufficient copies of this report are being distributed by FHWA memorandum to provide two copies to each FHWA Region, and three copies to each FHWA Division and State highway agency. Direct distribution is being made to the Division Offices. Additional copies for the public are available for the National Technical Information Service (NTIS), 5285 Port Royal Road, Springfield, Virginia 22161.

Byron N. Lord
Acting Director, Office of Engineering
and Highway Operations
Research and Development

NOTICE

Technical Report Documentation Page

1. Report No. FHWA-RD-90-111	2. PB93-227924	3. Recipient's Catalog No.
4. Title and Subtitle BLOWUP OF A CONCRETE PAVEMENT ADJOINING A RIGID STRUCTURE		5. Report Date August 1993 6. Performing Organization Code
7. Author(s) Arnold D. Kerr		8. Performing Organization Report No.
9. Performing Organization Name and Address University of Delaware Department of Civil Engineering DuPont Hall Newark, DE 19716		10. Work Unit No. (TRAIS) 3C4b2302 11. Contract or Grant No. DTFH61-88-P-00820
12. Sponsoring Agency Name and Address Office of Engineering and Highway Operations R&D Federal Highway Administration 6300 Georgetown Pike McLean, Virginia 22101-2296		13. Type of Report and Period Covered Final Report June 1988- Sept. 1988 14. Sponsoring Agency Code

15. Supplementary Notes

Contracting Officer's Technical Representative: Mr. William Kenis, HNR - 20

16. Abstract The main cause of concrete pavement blowups are axial compression forces induced into the pavement by a rise in temperature and moisture. Recent analyses by this writer and his students were based on the notion that blowups are caused by lift-off buckling of the pavement. The cases analyzed were: (1) continuously reinforced concrete pavement and (2) concrete pavement weakened by a traverse joint or crack.

The present paper contains an analysis of another case, when a long continuously reinforced concrete pavement adjoins a rigid structure, like a bridge abutment. The analysis is similar to the ones described above. The resulting formulation is non-linear and is solved exactly, in closed form. The obtained results are evaluated numerically and are compared with those of a long continuously reinforced pavement, in order to show the effect of the rigid structure on the pavement response.

17. Key Words Buckling of Pavements Rigid Pavements Concrete Pavements Blowup of Pavements	18. Distribution Statement No restrictions. This document is available to the public through the National Technical Information Service, Springfield, Virginia 22161

19. Security Classif. (of this report)	20. Security Classif. (of this page)	21. No. of Pages	22. Price
Unclassified	Unclassified	24	

Form DOT F 1700.7 (8-72) Reproduction of completed pag

SI* (MODERN METRIC) CONVERSION FACTORS

APPROXIMATE CONVERSIONS TO SI UNITS

Symbol	When You Know	Multiply By	To Find	Symbol
		LENGTH		
in	inches	25.4	millimeters	mm
ft	feet	0.305	meters	m
yd	yards	0.914	meters	m
mi	miles	1.61	kilometers	km
		AREA		
in²	square inches	645.2	square millimeters	mm²
ft²	square feet	0.093	square meters	m²
yd²	square yards	0.836	square meters	m²
ac	acres	0.405	hectares	ha
mi²	square miles	2.59	square kilometers	km²
		VOLUME		
fl oz	fluid ounces	29.57	milliliters	ml
gal	gallons	3.785	liters	l
ft³	cubic feet	0.028	cubic meters	m³
yd³	cubic yards	0.765	cubic meters	m³
NOTE: Volumes greater than 1000 l shall be shown in m³.				
		MASS		
oz	ounces	28.35	grams	g
lb	pounds	0.454	kilograms	kg
T	short tons (2000 lb)	0.907	megagrams	Mg
		TEMPERATURE (exact)		
°F	Fahrenheit temperature	5(F-32)/9 or (F-32)/1.8	Celcius temperature	°C
		ILLUMINATION		
fc	foot-candles	10.76	lux	l
fl	foot-Lamberts	3.426	candela/m²	cd/m²
		FORCE and PRESSURE or STRESS		
lbf	poundforce	4.45	newtons	N
psi	poundforce per square inch	6.89	kilopascals	kPa

APPROXIMATE CONVERSIONS FROM SI UNITS

Symbol	When You Know	Multiply By	To Find	Symbol
		LENGTH		
mm	millimeters	0.039	inches	in
m	meters	3.28	feet	ft
m	meters	1.09	yards	yd
km	kilometers	0.621	miles	mi
		AREA		
mm²	square millimeters	0.0016	square inches	in²
m²	square meters	10.764	square feet	ft²
m²	square meters	1.195	square yards	ac
ha	hectares	2.47	acres	mi²
km²	square kilometers	0.386	square miles	
		VOLUME		
ml	milliliters	0.034	fluid ounces	fl oz
l	liters	0.264	gallons	gal
m³	cubic meters	35.71	cubic feet	ft³
m³	cubic meters	1.307	cubic yards	yd³
		MASS		
g	grams	0.035	ounces	oz
kg	kilograms	2.202	pounds	lb
Mg	megagrams	1.103	short tons (2000 lb)	T
		TEMPERATURE (exact)		
°C	Celcius temperature	1.8C + 32	Fahrenheit temperature	°F
		ILLUMINATION		
lx	lux	0.0929	foot-candles	fc
cd/m²	candela/m²	0.2919	foot-Lamberts	fl
		FORCE and PRESSURE or STRESS		
N	newtons	0.225	poundforce	lbf
kPa	kilopascals	0.145	poundforce per square inch	psi

* SI is the symbol for the International System of Units. Appropriate rounding should be made to comply with Section 4 of ASTM E380.

(Revised August 1992)

BLOWUP OF A CONRETE PAVEMENT

ADJOINING A RIGID STRUCTURE

TABLE OF CONTENTS

LIST OF FIGURES

LIST OF TABLES

CHAPTER I. INTRODUCTION

There is general agreement that pavement blowups are caused by axial compression forces induced in the pavement by a rise in temperature and moisture. In 1984, analyses were presented for a long continuously reinforced concrete pavement (CRCP) and for a pavement with a transverse "hinge," based on the assumption that blowup is equivalent to lift-off buckling of the pavement.[1] A related analysis was presented in 1985.[2]

These two papers established the mechanism that leads to blowups. The resulting formulations are nonlinear, but it was possible to solve them exactly and in closed form. These analyses revealed a number of important parameters, like the pavement thickness h, the sliding frictional resistance at the interface of pavement and soil r_0^*, the effective flexural stiffness of the pavement $\underline{EI} = EI/(1-\nu^2)$, the coefficient of linear thermal expansion of pavement α, and the rotational and axial stiffness of the transverse joint or crack.

The present paper contains the analysis for another case; when a long continuously reinforced concrete pavement, that is subjected to temperature and moisture increases, adjoins a rigid structure, like a bridge abutment. The analysis is similar to the one used in reference 1. The derived closed form solutions are evaluated numerically. They are then compared with those of the jointless pavement analyzed previously, in order to show the effect of the rigid structure on pavement response.

CHAPTER II. CONCEPTUAL AND ANALYTICAL PRELIMINARIES

Consider a continuous concrete pavement that is adjoining an abutment as shown in figure 1(a). It is assumed at first that the pavement may rotate freely at the abutment but is constrained there from moving axially. This is the most unfavorable condition for blowup occurrence. The anticipated blowup mode is shown in figure 1(b). It is located near the abutment, because the "hinge," that may form by a badly spalled transverse joint or crack, shown in figure 2, weakens the pavement there and therefore reduces the temperature increase that may cause the shown blowup.

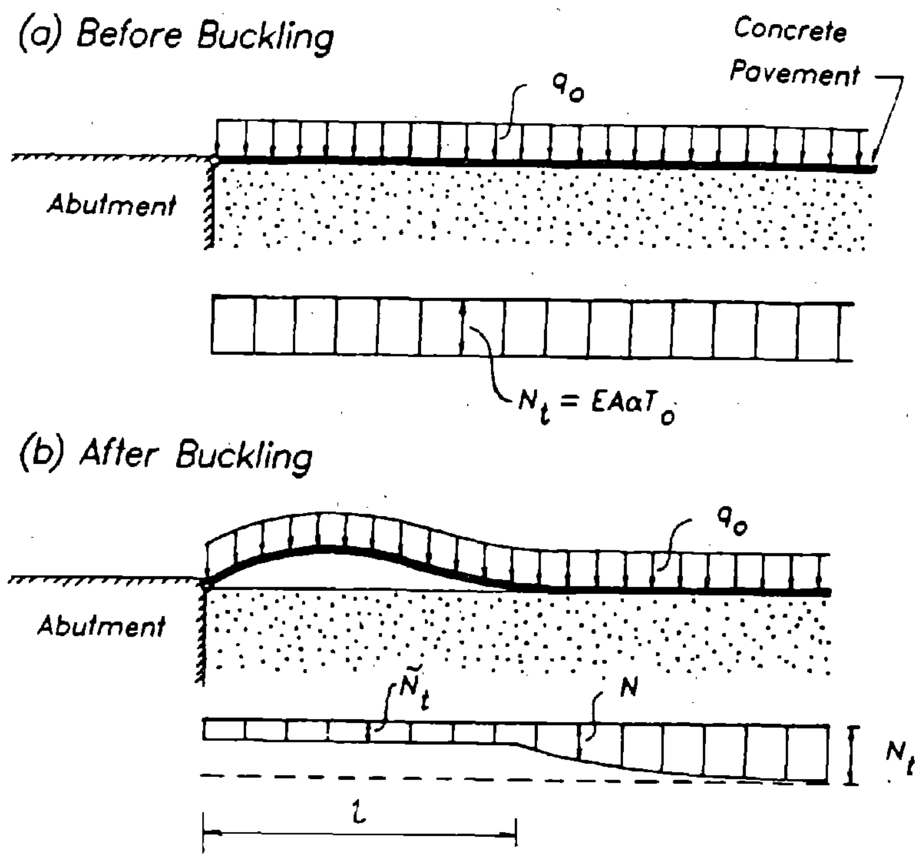

Figure 1. Problem under consideration.

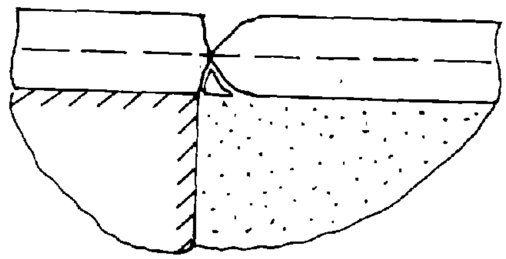

Figure 2. Spalled joint or crack at abutment

A moisture increase (or drop) in the concrete slab may be expressed by an equivalent temperature rise (or drop). Therefore, in the following only temperature changes will be discussed.

A uniform temperature increase above neutral induces, due to constrained expansions, a uniform axial compression force N_t, as shown in figure 1(a). For sufficiently large values of N_t the pavement may buckle upward. Then in the *lift-off region of length l*, part of the constrained expansions are released. This results in a drop of the axial force in the lift-off region to $\tilde{N}_t$. In the *adjoining region*, due to resistance to axial displacements at the interface of pavement and base, the constrained axial expansions vary; so does the axial force $\tilde{N}_t < N < N_t$, as shown in figure 1(b).

In the following analysis, the concrete pavement is replaced by a beam of rectangular cross section. Because the ratio of pavement width to thickness is generally $b/h > 20$, for numerical evaluations the bending stiffness is assumed to be $\mathbf{EI} = EI/(1-\nu^2)$, to account for plate action. The x-axis is placed through the centroid as reference axis. Note that x is a Lagrange coordinate.

Graphs of the axial shearing resistance at the interface of pavement and base, caused by axial displacements, are shown in figure 3. The test results

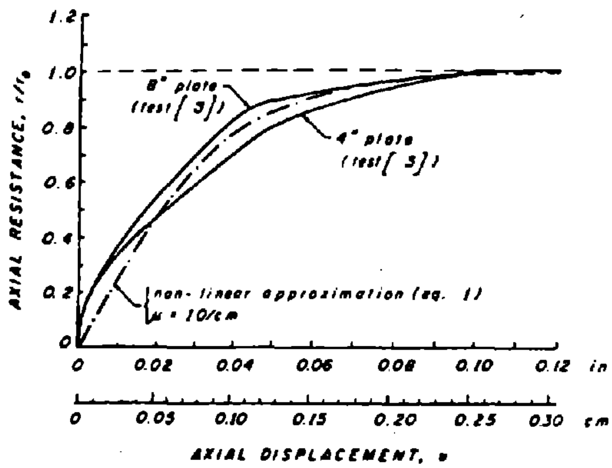

Figure 3. Axial resistance-displacement response.

are shown as solid curves.[3] In the following this response is represented by the non-linear relation:

$$r(x) = r_0 tgh[\mu u(x)] \tag{1}$$

shown as the dash-dot-dash curve. The parameter r_o is the sliding frictional resistance and μ is a second parameter for fitting the analytical expression with the test data. The shown curve is for μ = 10/cm. Note that $r_o = br_o^*$ where b is the width of pavement under consideration and r_o^* is the sliding frictional resistance per unit area. Values for r_o^*, based on test data from references 3 and 4 are shown in figure 4. Although the resistance response shown in figure 3 is non-elastic, the use of relation (1) is justified because during blowup the axial displacements are monotonically increasing.

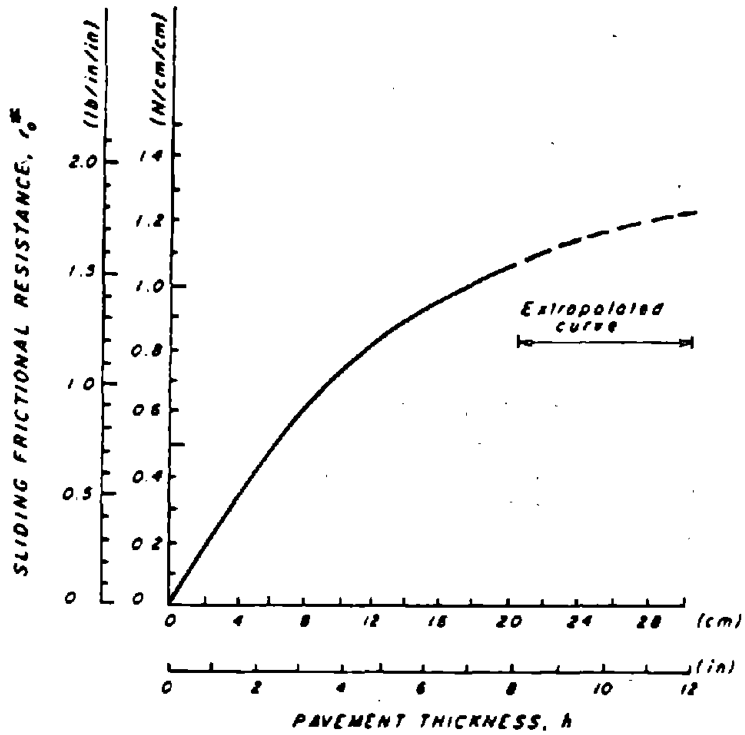

Figure 4. Sliding frictional resistance as a function of pavement thickness (based on test data presented in references 3 and 4).

In the following analysis it is assumed that the pavement is subjected to a uniform temperature increase, T_0 above neutral and a uniformly distributed own weight, q_0, per unit length of pavement axis. Because the vertical deflections in the adjoining region are very small, it is assumed that the base is rigid. As shown in reference 5 for a related problem, this appears to be justified. Furthermore it is assumed that prior and during buckling the response of the concrete pavement is elastic.

An important feature of the formulation to be used is that, although the resulting differential equations are non-linear, they can be solved in closed form. The solution yields the post-buckling displacements and axial forces in the pavements. The anticipated results are shown schematically in figure 5.

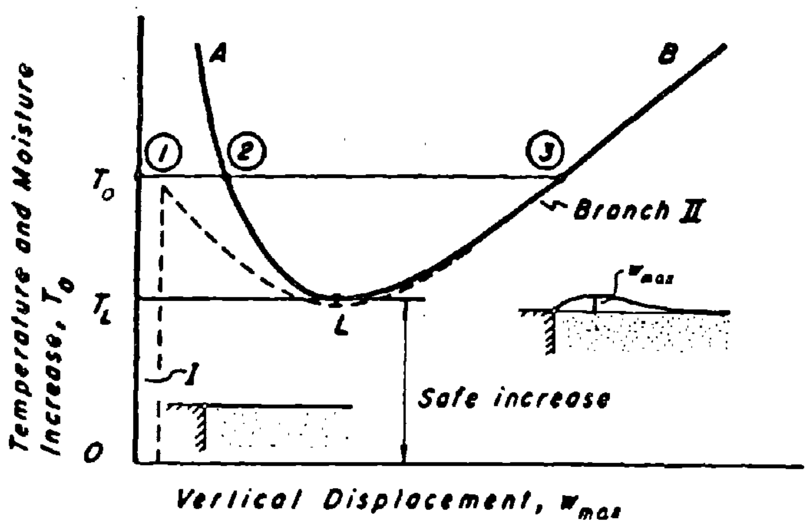

Figure 5. Typical equilibrium branches for pavement.

Each point on the shown equilibrium branches corresponds to an equilibrium configuration of the pavement. Branch I corresponds to the straight unbuckled equilibrium states and Branch II to the vertically deformed states. When the pavement is subjected to a temperature increase $T_o < T_L$, there exists only the straight (stable) equilibrium configuration. However, to a temperature increase $T_o > T_L$, there correspond three states of equilibrium: The (stable) straight state ①, the (unstable) vertically deformed configuration ② on branch AL, and the (stable) vertically deformed configuration ③ on branch LB. Thus, when the pavement buckles at a temperature increase $T_o > T_L$, it will move to the deformed equilibrium configuration ③ on branch LB.

A static stability analysis of a concrete pavement subjected to axial compression forces consists of two parts: (1) The determination of all equilibrium states and (2) the investigation of which of the determined equilibrium states are stable and which are not. From the nature of the post-buckling equilibrium branches, and their stability, it follows that the "safe range" of temperature increases to prevent pavement buckling may be determined solely from the post-buckling equilibrium branch, as shown in figure 5. It is:

$$0 < T_o < T_L \qquad (2)$$

This concept was used in the two earlier analyses, references 1 and 2, and will be used in the following study.

Because pavements are usually not "perfectly" straight, it is of interest to know the effect of vertical geometric imperfections on the safe temperature range. An equilibrium branch for relatively small imperfections is shown schematically in figure 5, as a dashed line. Noting that the T_L-value for this branch is very close to the T_L-value for the perfectly straight pavement it is concluded that criterion (2) is also valid for a pavement with small vertical imperfections.

CHAPTER III. ANALYSIS OF PAVEMENT

Following the methodology developed in references 1 and 2, the equilibrium states of the vertically deformed pavement, shown in figure 1(b), are described by the differential equations:

$$\left.\begin{aligned} (\overline{EI}w_1'')'' - [EA(\epsilon_1 - \alpha T_o)w_1']' &= q_o \qquad &(a)\\ [EA(\epsilon_1 - \alpha T_o)]' &= 0 \qquad &(b)\end{aligned}\right\} \quad 0 < x < l \qquad (3)$$

and

$$\left.\begin{aligned} w_a(x) &\equiv 0 \qquad &(a)\\ -(EAu_a')' + r_o tgh(\mu u_a) &= 0 \qquad &(b)\end{aligned}\right\} \quad l < x < \infty \qquad (4)$$

The corresponding boundary and matching conditions are:

$$w_1(0) = 0 \quad ; \quad w_1''(0) = 0 \quad ; \quad u_1(0) = 0 \qquad (5)$$

$$\left.\begin{aligned} w_1(l) = 0 \quad ; \quad w_1'(l) = 0 \quad ; \quad w_1''(l) = 0 \\ u_1(l) = u_a(l) \quad ; \quad u_1'(l) = u_a'(l)\end{aligned}\right\} \qquad (6)$$

and the regularity condition:

$$\lim_{x\to\infty}[u_a(x), u_a'(x)] \to 0 \qquad (7)$$

The above formulation consists of three non-linear differential equations and nine conditions for the determination of the eight integration constants (4 for w_1, 2 for u_1, and 2 for u_a) and the lift-off length l.

In equations (3) to (7), $u_n(x)$ and $w_n(x)$ are the axial and vertical displacements at point x of the pavement reference axis x, the subscript n denotes the pavement region, "1" refers to the buckled region and "a" refers to the adjoining region,

$$\epsilon_n = u_n' + \frac{1}{2} w_n'^2$$

$(\ )' = d(\ )/dx$, q_o is the constant pavement weight per unit length, r_o and μ are the axial resistance parameters, as defined by relation (1). E is Young's modulus of pavement, A is its cross-sectional area, and EI is its bending stiffness. α is the coefficient of linear thermal expansion of pavement and T_o is the uniform temperature increase in the pavement above the "neutral" temperature.

The corresponding axial forces, bending moments, and shearing forces in the pavement are:

$$\left.\begin{aligned} N_n(x) &= - EA(\epsilon_n - \alpha T_o) \quad ; \quad N > 0 \text{ compression} \\ M_n(x) &= - \overline{EI}w_n'' \\ V_n(x) &= - (\overline{EI}w_n'')' + EA(\epsilon_n - \alpha T_o)w_n' \end{aligned}\right\} \tag{8}$$

Next, the formulation in equations (3) to (7) is solved. The differential equations in (3) and (4) are *non-linear*. However, since equation (3a), when integrated, yields:

$$EA(\epsilon_1 - \alpha T_o) = \text{const.} = -\tilde{N}_t \qquad 0 < x < l \tag{9}$$

the equation (3b) reduces, for $\overline{EI}$ = constant, to

$$\overline{EI}w_1'''' + \tilde{N}_t w_1'' = q_o \qquad ; \qquad 0 < x < l \tag{10}$$

a linear ordinary differential equation with *constant* coefficients. The differential equation (4b) is also *non-linear*. However, since it is of the form u" - F[u] it may be easily solved. These analytical features make it possible to solve the above non-linear formulation in closed form.

According to the equations in (8), the left-hand side of equation (9) is the axial force in the buckled region. It is denoted by $-\tilde{N}_t$. Thus, the axial compression force in the buckled region 0 < x < 1 is $\tilde{N}_t$ and is constant in this domain.

The general solution of equation (10) is

$$w_1(x) = A_1\cos\lambda x + A_2\sin\lambda x + A_3 x + A_4 + \frac{q^*}{2\lambda^2}x^2 \tag{11}$$

where

$$\lambda = \sqrt{\tilde{N}_t / \overline{EI}} \qquad ; \qquad q^* = q_o / \overline{EI} \tag{12}$$

Since for the problem under consideration $\tilde{N}_t > 0$, it follows that λ is a real number.

The integration constants A_1 to A_4 are determined from the first two conditions in equation (5) and in equation (6). They are:

$$\left.\begin{aligned} A_1 &= \frac{q^*}{\lambda^4} \quad ; \quad A_2 = \frac{q^*}{\lambda^4}\,\frac{\lambda l\sin\lambda l + \cos\lambda l - (\lambda l)^2/2 - 1}{\lambda l\cos\lambda l - \sin\lambda l} \\ A_3 &= \frac{q^*}{\lambda^3}\,\frac{\lambda l(\sin\lambda l - \lambda l\cos\lambda l/2) + \cos\lambda l - 1}{\lambda l\cos\lambda l - \sin\lambda l} \quad ; \quad A_4 = -\frac{q^*}{\lambda^4} \end{aligned}\right\} \tag{13}$$

when $\operatorname{tg}\lambda l \neq \lambda l$.

Substituting the obtained $w_1(x)$ into the condition $w_1''(l) = 0$ given in equation (6), it follows that it is satisfied when:

$$2(1 - \cos\lambda l) = \lambda l \sin\lambda l \tag{14}$$

The non-zero roots of this equation are:

$$\lambda l = 2\pi,\ 8.987,\ \ldots \tag{15}$$

It may be shown that the first root 2π corresponds to the deformation shape shown in figure 1(b). This is the condition for the determination of l. Namely:

$$l = \frac{2\pi}{\lambda} = 2\pi\sqrt{\frac{EI}{\tilde{N}_t}} \tag{16}$$

With $\lambda l = 2\pi$, the constants A_1 to A_4 simplify and $w_1(x)$ becomes:[6]

$$w_1(x) = \frac{q^*}{\lambda^4}\left[\cos\frac{2\pi x}{l} - \pi \sin\frac{2\pi x}{l} - 2\pi^2\frac{x}{l} + 2\pi^2\left(\frac{x}{l}\right)^2 - 1\right] \tag{17}$$

The above expression for $w_1(x)$, in conjunction with condition (16), $\lambda = 2\pi/l$, still contain the unknown $\lambda = \sqrt{\tilde{N}_t/EI}$. It is determined in the following as part of the solution of the remaining equations in the foregoing formulation; namely those for $u_1(x)$ and $u_a(x)$.

The first integral of equation (3b), equation (9), is the *non-linear* differential equation of the first order:

$$EA\left(u_1' + \frac{1}{2}w_1'^2 - \alpha T_o\right) = -\tilde{N}_t \qquad 0 < x < l \tag{9'}$$

Since at this point of the analysis $w_1(x)$ is a known function, given in equation (17), the above equation reduces to the linear ordinary differential equation for u_1

$$u_1'(x) = \left(\alpha T_o - \frac{\tilde{N}_t}{EA}\right) - \frac{1}{2}w_1'^2(x) \tag{18}$$

Integrating it from 0 to x, and noting that according to equation (5) $u_1(0)=0$, the following is obtained:

$$u_1(x) = \left(\alpha T_o - \frac{\tilde{N}_t}{EA}\right)x - \frac{1}{2}\int_0^x w_1'^2(\xi)d\xi \tag{19}$$

Because EA = constant and $w_a(x) \equiv 0$, equation (4b) reduces to the *non-linear* differential equation:

$$EAu_a'' = r_o \mathrm{tgh}[\mu u_a(x)] \qquad l < x < \infty \tag{20}$$

This equation is a special case of $u''(x) - F[u(x)]$; a well known equation from non-linear vibration theory. It is solved, in closed form, by noting the identity $2u'' = d(u'^2)/du$. With it, equation (20) may be written as:

$$d(u_a'^2) = \frac{2r_o}{EA} \mathrm{tgh}(\mu u_a) du_a \tag{21}$$

Integrating it yields:

$$u_a'^2(x) = \frac{2r_o}{EA} \int \mathrm{tgh}(\mu u_a) du_a + B_1$$

$$= \frac{2r_o}{EA} \ln\{\cosh[\mu u_a(x)]\} + B_1 \tag{22}$$

Because the regularity condition, equation (7), it follows that $B_1 = 0$. Thus:

$$u_a'(x) = (\pm) \sqrt{\frac{2r_o}{\mu EA} \ln\{\cosh[\mu u_a(l)]\}} \tag{23}$$

The positive sign is retained, because the anticipated axial displacements $u_a(x)$ for $x > 0$ will be negative, decreasing in magnitude with increasing x.

Substituting $u_1'(x)$ given in (18) and $u_a'(x)$ given in (23) into the fifth condition of (6), $u_1'(l) = u_2'(l)$, and noting that according to the second condition of (6) $w_1'(l) = 0$, we obtain:

$$\alpha T_o - \frac{\tilde{N}_t}{EA} - \sqrt{\frac{2r_o}{\mu EA} \ln\{\cosh[\mu u_a(l)]\}} = 0 \tag{24}$$

According to equation (6) the condition $u_1(l) = u_a(l)$ still has to be satisfied. The expression $u_1(l)$ is obtained by integrating equation (18) from 0 to l. Since $u_1(0) = 0$ it follows that:

$$u_1(l) = \left(\alpha T_o - \frac{\tilde{N}_t}{EA}\right) l - \frac{1}{2} \int_0^l w_1'^2(x) dx \tag{25}$$

Eliminating $u_a(l)$ in equation (24) using the remaining matching condition $u_a(l) - u_1(l)$ and then utilizing equation (25), we obtain:

$$\alpha T_o - \frac{\tilde{N}_t}{EA} = \sqrt{\frac{2r_o}{\mu EA}\ \ln\left[\left[\cosh\left\{\mu\left[\left[\left(\alpha T_o - \frac{\tilde{N}_t}{EA}\right) l - J\right]\right\}\right]\right]} \tag{26}$$

where:[6]

$$J = \frac{1}{2}\int_o^l w_1'^2(\xi)d\xi = 0.00008715q*^2 l^7 . \tag{27}$$

The solution for the problem shown in figure 1 is just completed. For a given concrete pavement (i.e. for known values of E, A, I, ν, α, q_o, r_o and μ) the numerical evaluation of the obtained solution consists of the following steps: Choose a positive value of $\tilde{N}_t$ and determine the corresponding $\lambda = \sqrt{\tilde{N}_t/\overline{EI}}$ and then $l = 2\pi/\lambda$. For this (λ, l) pair calculate the corresponding T_o value from equation (26) in conjunction with equation (27). The corresponding value of w_{max} is calculated from equation (17), by first forming $dw_1/dx = 0$ which yields $x/l = 0.3464$ and then by substituting this value into $w_1(x)$. The result is:

$$w_{max} = -0.005532\ q_o l^4 / \overline{EI} \tag{28}$$

These steps are repeated for a range of N_t values of interest.

CHAPTER IV. NUMERICAL EVALUATION AND DISCUSSION OF RESULTS

The numerical evaluation of the derived solution was performed for a pavement of constant rectangular cross section, for pavement thicknesses h = 6 in (15 cm), 8 in (20 cm), 10 in (25 cm), 12 in (30 cm) and 14 in (35 in). It may be easily verified that the obtained results are independent of the pavement width b because r_0, A, I, and $\bar{N}_t$ are linearly varying with b. The chosen pavement parameters are:

$$\left.\begin{array}{ll} E = 4.35 \times 10^6 \text{ lb/in}^2 \ (3{,}000 \text{ kN/cm}^2) \quad ; & \nu = 0.3 \\ \alpha = 0.5 \times 10^{-5}/^\circ F \ (0.9 \times 10^{-5}/^\circ C) \quad ; & \gamma = 150 \text{ lb/ft}^3 \ (23.6 \text{ kN/m}^3) \end{array}\right\} \tag{29}$$

γ being the unit weight of the pavement material.

Since generally the reinforcement ratio in the pavement is very low (0.5 to 0.75 percent), and it is usually placed near the mid-plane of the cross section, the effect of the reinforcing bars was neglected when calculating the cross-sectional area A and the effective flexural stiffness $\bar{EI}$ - EI/(1 - ν2).

The sliding frictional resistance values r_0^* at the interface of pavement and base per unit length and unit width of pavement, as defined in equation (1), was determined from the test data in reference 3 and are shown in table 1.

Table 1. Dependence of r_0^* on h.[3]

h	in	6	8	10	12	14
	(cm)	(15)	(20)	(25)	(30)	(35)
r_o^*	lb/in²	1.34	1.55	1.65	1.74	1.81
	(N/cm²)	(0.92)	(107)	(1.14)	(1.20)	(1.25)

To closely approximate the test data in references 3 and 4, it was assumed that μ = 25.4/in (10/cm) for all five pavement thicknesses, as shown in figure 3.

The obtained solution was evaluated for the above parameters. The results are shown in figure 6. Note the drop of the axial force in the buckled region. Also note that the magnitude of the lift-off displacement, w_{max} depends on the temperature increase T_0 at which buckling takes place; the higher the temperature increase the larger is w_{max}. For example for a pavement with h = 25 cm, to an increase $T_0 = T_L$ = 56∘C there corresponds a w_{max} = 36 cm where as to T_0 = 65 ∘C there corresponds $w_{max} \approx$ 75 cm; thus more then twice as large.

To show the effect of pavement thickness h on the safe tempture increases above neutral, these results are plotted in figure 7 as a solid line. Also shown in this figure, as a dashed line, is the corresponding curve.

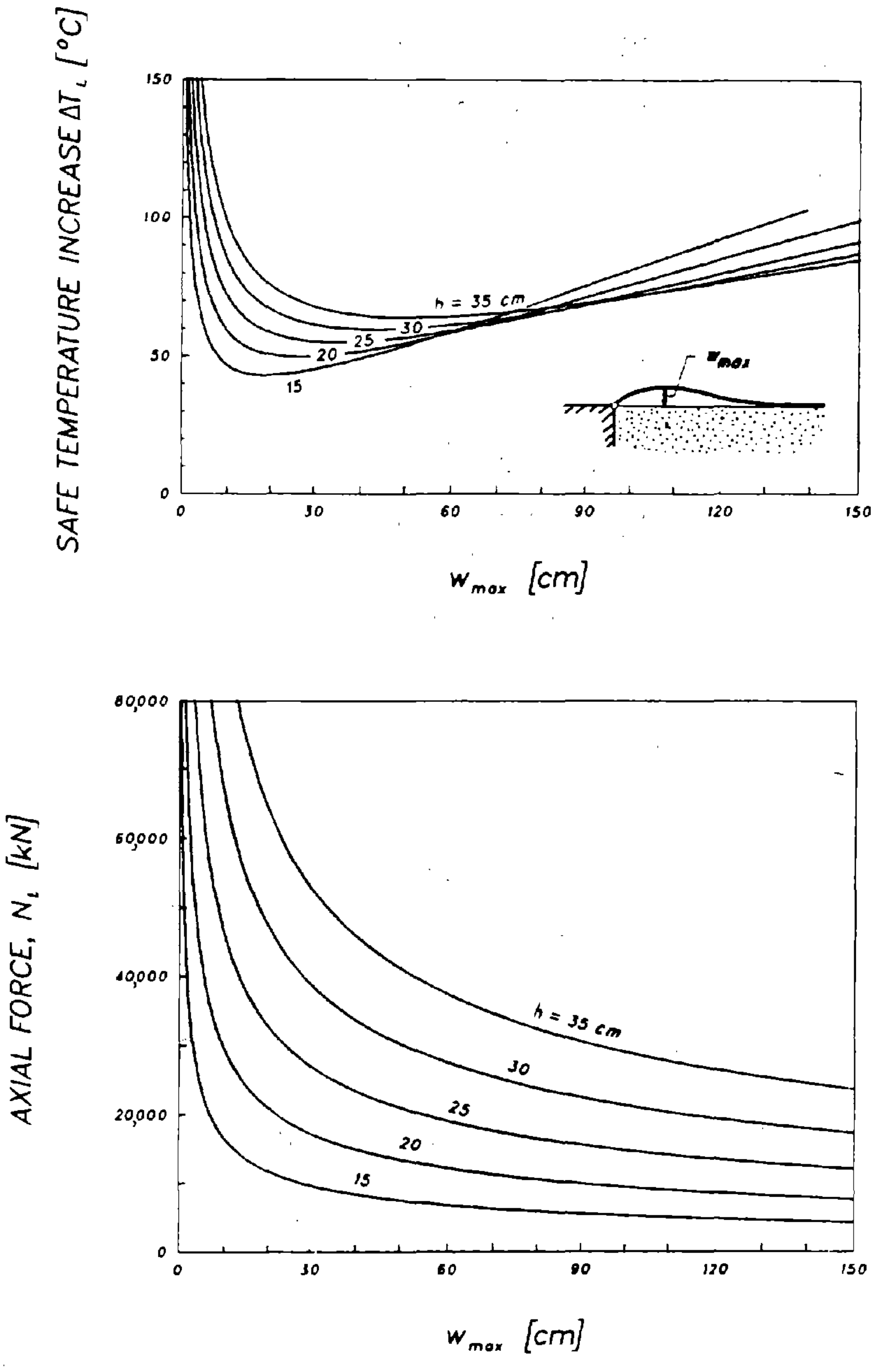

Figure 6. Equilibrium branches and axial forces in pavement. (For the determination of $\tilde{N}_L$, b= 24 ft (725 cm) was used.)

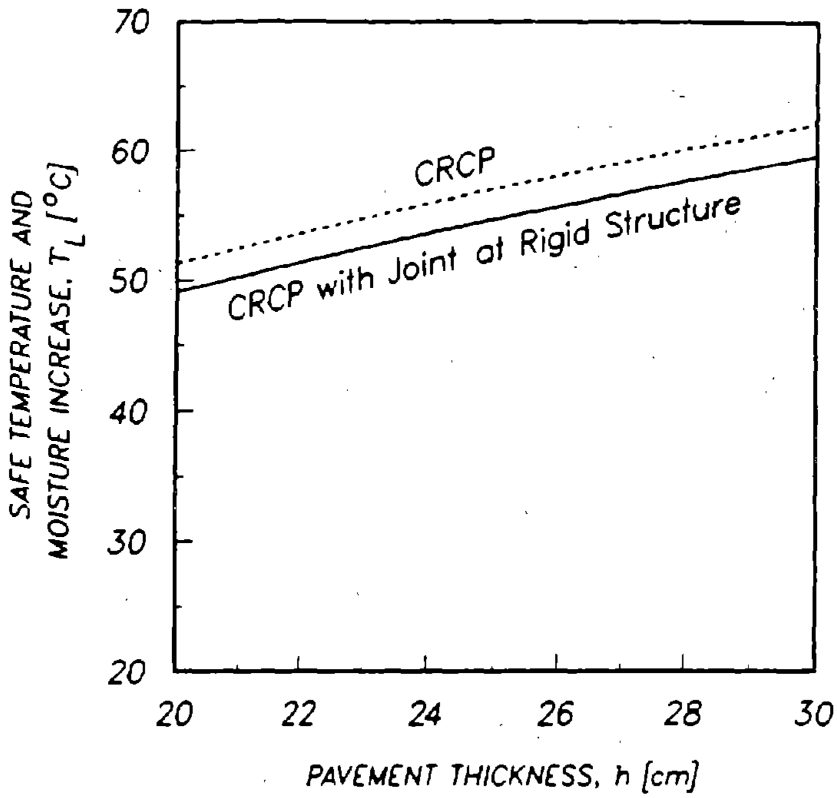

Figure 7. Dependence of T_L on pavement thickness h.

for the continously reinforced concrete pavement (CRCP) far away from the bridge abutment as determined in references 1 and 2. Note the efect of the hinge and "rigid" abutment on the safe temperature increase.

Next, consider the case when the pavement that was rigidly attached to the abutment exhibits, after a time, a transverse crack at this location. This will correspond to the case shown in figure 1, but with rotational resistance in the hinge that will depend on the degree of spalling, as indicated in figure 2. This resistance will increase the safe temperature increase above the values of the solid curve shown in figure 7.

The axial compression force that a CRCP will generate is $N_t = EA\ \alpha\ T_0$. For the pavement parameters used above, h= 10 in (25 cm) and b= 24 ft (725 cm), this corresponds to an axial compression force, per °C, of:

$$\frac{N_t}{T_0} = EA\alpha = 3{,}000 \times 25 \times 725 \times 0.9 \times 10^{-5} \doteq 490\ \mathrm{kN/°C}$$

This rather large compression force (per °C) demonstrates the importance of the *neutral* temperature on pavement blows. The higher the *neutral* temperature the less likely is the possibility that blowup will occur. Note, however, that although a higher *neutral* temperature may prevent blowups, it will lead (in CRCP's) to higher axial tensile forces in the pavement during the winter, that may cause pavement ruptures. This indicates that the construction season has an effect on the pavement response.

Some pavement engineers are of the opinion that the shearing resistance at the interface contributes to the formation of transverse cracks and thus should be minimized; for example, by placing plastic sheets at the interface. To establish this effect on blowups, the obtained solution was evaluated numerically for different values of the sliding frictional resistance parameter, r_o^*, without changing the other parameters. The results are shown in figure 8. Note that, according to the above analysis and those of

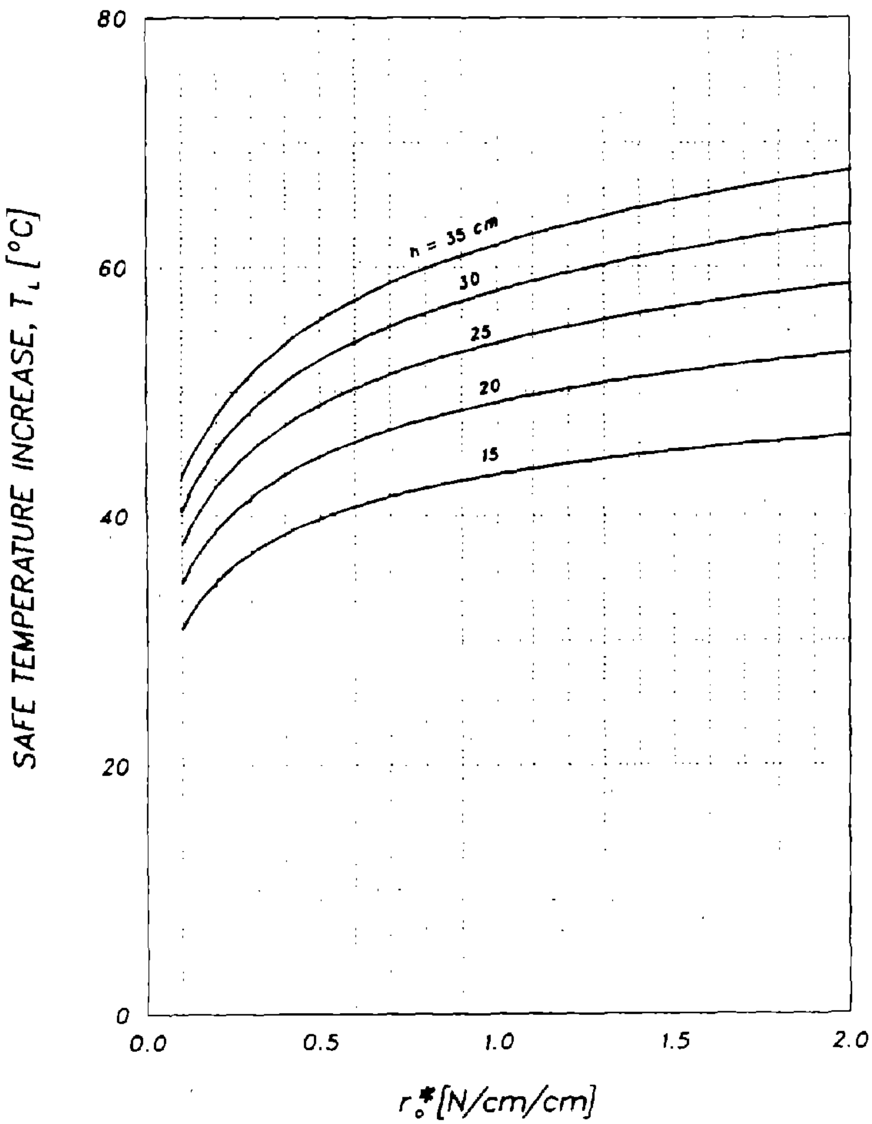

Figure 8. Dependence of T_l on r_o^*

references 1 and 2, a reduction of this resistance, r_0^*, also reduces the safe temperature range, $0 < T < T_L$, and thus has an adverse effect on pavement blowups. For preventing blowups, the sliding frictional resistances should be as high as possible.

To reduce the axial forces that a concrete highway pavement will exert on a bridge pier, short section of a black top slab is often inserted between the pavement and the abutment. This allows the end zone of the pavement, during periods of high temperatures, to expand toward the bridge, preventing the build up of high compression forces in the vicinity of the bridge abutment. However, the continuous expansion and contraction of the pavement in this region creates maintenance problems, especially when the shearing resistance between pavement and subgrade is very small.

REFERENCES

1. A. D. Kerr, and P. J. Shade, "Analysis of Concrete Pavement Blowups," *Acta Mechanica*, Springer Verlag, Vienna, Austria, Vol. 52, 1984.

2. A. D. Kerr, and W. A. Dallis, Jr., "Blowup of Concrete Pavements," *Journal of Transportation Engineering*, ASCE, Vol. 111, No. 1, 1985.

3. L. W. Teller, and E. C. Sutherland, "Observed Effects of Variations in Temperature and Moisture on the Size, Shape and Stress Resistance of Concrete Pavement Slabs," *Public Roads*, Public Roads Administration, Washington, D.C., Vol. 16, Nr. 9, 1935.

4. E. F. Kelley, "Application of the Results of Research to the Structural Design of Concrete Pavements," *Public Roads*, Public Roads Administration, Washington, D.C., Vol. 20, Nr. 6, 1939.

5. Y. M. El-Aini, "Effect of Foundation Stiffness on Track Buckling," *Journal of the Engineering Mechanics Division*, ASCE, Vol. 102, EM 3, 1976.

6. A. D. Kerr, "An Improved Analysis for Thermal Track Buckling," *International Journal for Non-Linear Mechanics*, Pergamon Press, Vol. 15, 1980, page 107.

*U.S. G.P.O.:1993-343-273:80069